1992

Kinematics of fault-related folding in a duplex, Lost River Range, Idaho, U.S.A.

Christopher A. Hedlund
Lehigh University

AUTHOR:

Hedlund, Christopher A.

TITLE:

Kinematics of Fault-Related Folding In a Duplex, Lost River Range, Idaho, U.S.A.

DATE: January 17, 1993

Kinematics of fault-related folding in a duplex, Lost River Range, Idaho, U.S.A.

by

Christopher A. Hedlund

A Thesis

Presented to the Graduate Committee

of Lehigh University

in Candidacy for the Degree of

Master of Science

in

Geological Sciences

Lehigh University

1992

This thesis is accepted and approved in partial fulfillment of the requirements for the degree of Master of Science.

10 December 1992
(date)

Professor in Charge

Chairman of Department

ACKNOWLEDGEMENTS

The author acknowledges David J. Anastasio for his guidance and advice in all aspects of the research summarized in this paper. This manuscript has benefitted from discussions with Michael A. Krol and M. Scott Wilkerson, and from reviews by David J. Anastasio, Donald M. Fisher, Anne S. Meltzer, and Ken P. Kodama. The author acknowledges the facilities, resources, and personel of the Department of Earth and Environmental Sciences at Lehigh University.

Research summarized in this manuscript was supported by NSF grant EAR-9017334 to David J. Anastasio and Donald M. Fisher, and by grants from the American Association of Petroleum Geologists, the Geological Society of America, and Sigma Xi to the author. The author acknowledges Richard W. Allmendinger for the use of Stereonet software, and Donald M. Fisher and M. Brooks Clark for providing incremental strain software.

TABLE OF CONTENTS

LIST OF FIGURES

ABSTRACT

The Doublespring duplex, located in the Lost River Range of Idaho, is a Sevier age fault-related fold complex in massive limestones of the Upper Mississippian Scott Peak Formation. Folds within the duplex closely resemble fault-bend fold geometries, with open interlimb angles and shallow bed cutoffs. Narrow, widely spaced bedding-parallel shear zones with well developed pressure solution cleavage alternate with massive, relatively undeformed layers on fold limbs. Shear zones are developed only on the limbs of anticlines, and have similar but unique morphologies on each of three different folds. Incremental strain histories reconstructed from antitaxial fibrous overgrowths and veins constrain the kinematics of folding. Shear zones experience flexural flow toward pins near axial surfaces, while adjacent massive layers experience rotation through a fixed extension direction. Late fiber increments that are nearly cleavage-parallel indicate that the fabric developed late in the strain history. The absence of footwall synclines and morphological differences in shear zones from adjacent folds suggest that faulting preceded folding. Kinematic histories of folds that have experienced different translational histories are identical, and are not compatible with strain histories predicted from kinematic models of fault-bend folding. Shear zone development and fiber growth is instead interpreted to occur during low amplitude fixed-hinge buckling in response to resistance to initial translation of the thrust sheet.

Fault-bend folding with mobile axial surfaces occurred with translation of the thrust sheets once the initial resistance to translation was overcome, and left no textural record.

INTRODUCTION

THE complex relationship between faulting and folding in foreland fold-thrust belts has intrigued structural geologists for decades (ie. Willis, 1893; Rich, 1934; Boyer, 1986). Currently, fault-related folds are generally recognized to be either 1) fault-bend folds which form in response to displacement on a non-planar or stepped fault surface (Rich, 1934; Suppe, 1983), 2) fault-propagation folds which accommodate shortening above a propagating thrust ramp (Suppe and Medwedeff, 1984; Mitra, 1990; Suppe and Medwedeff, in press), or 3) décollement folds which form above a flat thrust segment (Dahlstrom, 1970; Jamison, 1987). The geometry and kinematics of fault-related folding are intimately related; fold geometry depends in part on the orientation and distribution of shear during folding, while the details of fold kinematics are affected by the geometry of the fault. Kinematic models predicting the geometric evolution of fault-related folds (Sanderson, 1982; Suppe, 1983; Suppe and Medwedeff, 1984) closely simulate the geometry of natural structures and provide the basis for geometric

reconstructions of fold-thrust structures.

While the geometries of natural fault-related folds have been studied extensively, only recently have empirical studies begun to place constraints on the kinematics of fault-related folding. Beutner *et al.* (1988) interpreted incremental strain data from the Hamburg sequence to represent folding by vertical simple shear at axial surfaces fixed in a footwall ramp. More recently, Fischer *et al.* (1992) and Fisher and Anastasio (in press) have presented evidence for a fixed-hinge buckling origin for asymmetric fault-related folds in the Sevier thrust belt based on the distribution of structural fabrics and incremental strain histories, respectively. The importance of kinematics in the interpretation, evaluation, and reconstruction of geologic structures is universally recognized (ie. Geiser, 1988). This paper presents results from a kinematic analysis of fault-related folds in a duplex using incremental strain analysis of syntectonic fibers in pressure shadows and veins. These results give insights into the partitioning of fold mechanisms in a layered sequence and provide constraints on the timing and distribution of deformation during fault-related folding.

GEOLOGIC SETTING

The Lost River Range is the westernmost of a series of NNE-SSW trending ranges

in the extension of the Basin and Range province north of the Snake River Plain in south-central Idaho, U.S.A. The range is bound to the west by the seismically active (Crone and Haller, 1991, and references therein) Lost River Fault, and to both the east and west by structural basins related to Miocene-Holocene extension (Ross, 1947; Baldwin, 1951; Mapel *et al.,* 1965). The northern Lost River Range (Fig. 1) is a first-order synclinoria exposing a thick prograding carbonate bank complex consisting of the Upper Mississippian Middle Canyon (~200 m), Scott Peak (700 m), South Creek (~160 m), and Surrett Canyon (~300 m) formations, and the Lower Pennsylvanian Arco Hills (~30 m), Bluebird Mountain (100 m), and Snaky Canyon (1100+ m) Formations (Mamet *et al.,* 1971; Rose, 1977; Skipp *et al.,*1979). The structure considered in this study occurs in the Scott Peak Formation, a massive limestone unit consisting of biomicrite with occasional chert nodule-rich beds. A tapered wedge (1220 to 30 m thick, ~225 m at Doublespring) of Lower Mississippian flysch derived from the Antler highlands to the west, the McGowan Creek Formation, separates the upper Paleozoic carbonate shelf sequence from the underlying lower Paleozoic mixed carbonate/clastic sequence (Mapel *et al.,* 1965; Skipp *et al.,* 1979). The McGowan Creek Formation serves as a regional décollement above which numerous eastward-vergent, NNE-SSW trending fault-related folds formed in the upper Paleozoic sequence during the Sevier Orogeny (Fisher and Anastasio, in press).

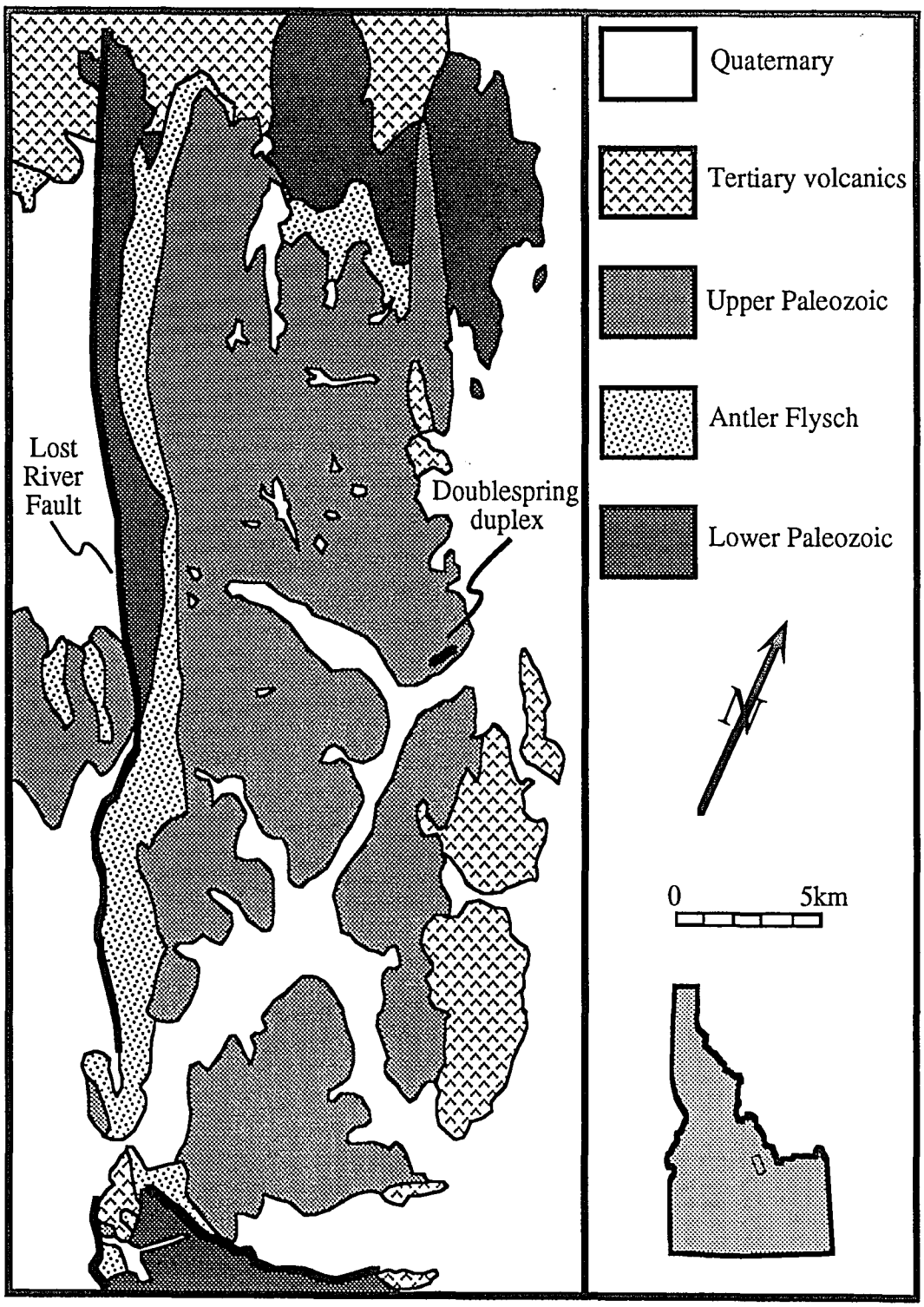

Figure 1. Geologic map of the northern Lost River Range, Idaho, showing location of the Doublespring duplex. The Lost River Range is a synclinoria exposing primarily an Upper Paleozoic carbonate bank complex that has been shortened by NW-SE trending Sevier-age fault-related folds.

THE DOUBLESPRING DUPLEX

Geometry

The structure exposed at Doublespring (Fig. 1) consists of a complexely folded sequence of massive limestone on the homoclinally dipping (25° towards N70°E) flank of a larger-order structure (Fig. 2a). Stratigraphic cutoff geometries and axial surface relationships indicate that folds are closely related to underlying imbricate thrust ramps and constrain the geometry of the faults. These constraints provide the basis for a line-length and area balanced cross section of the Doublespring structure (Fig. 3). The Doublespring structure is interpreted to be a hinterland dipping duplex (Boyer and Elliott, 1982) where two imbricates converge at a leading branch line to form a single horse. A minimum of 50 m of shortening is accommodated by displacement on these two imbricate thrusts.

Three anticlinal folds in the Doublespring duplex (Figs. 2b & 3) are the focus of the kinematic analysis, and are henceforth referred to as the upper, middle, and lower folds. These folds are curved or concentric (rather than kinked), parallel, and cylindrical in geometry (Fig. 4), with open interlimb angles ranging from 130° to 145°. The upper fold is a leading edge fold that has experienced little translation such that the

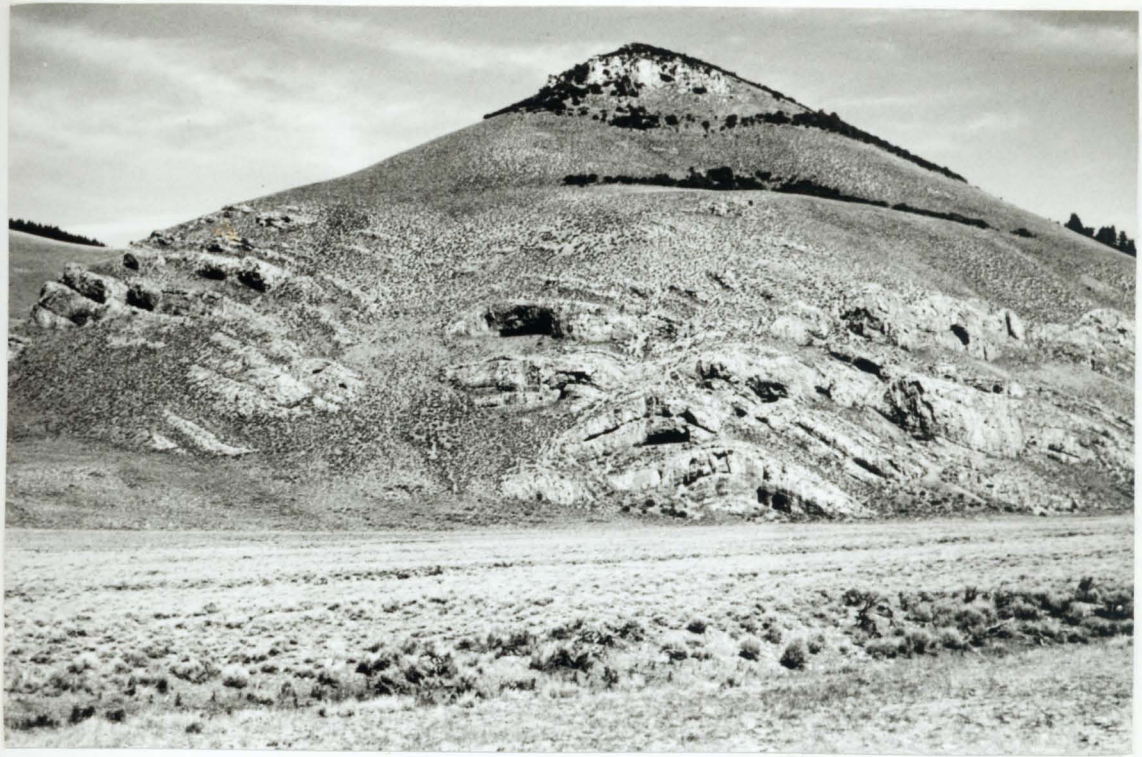

Figure 2a. Photograph of the Doublespring duplex. View is toward N70°W, looking down the fold axis. Field of view is approximately 225 meters.

Figure 2b. Close-up photograph of the three anticlinal folds in the Doublespring duplex. View is toward N70°W, looking down the fold axis. Field of view is approximately 50 meters.

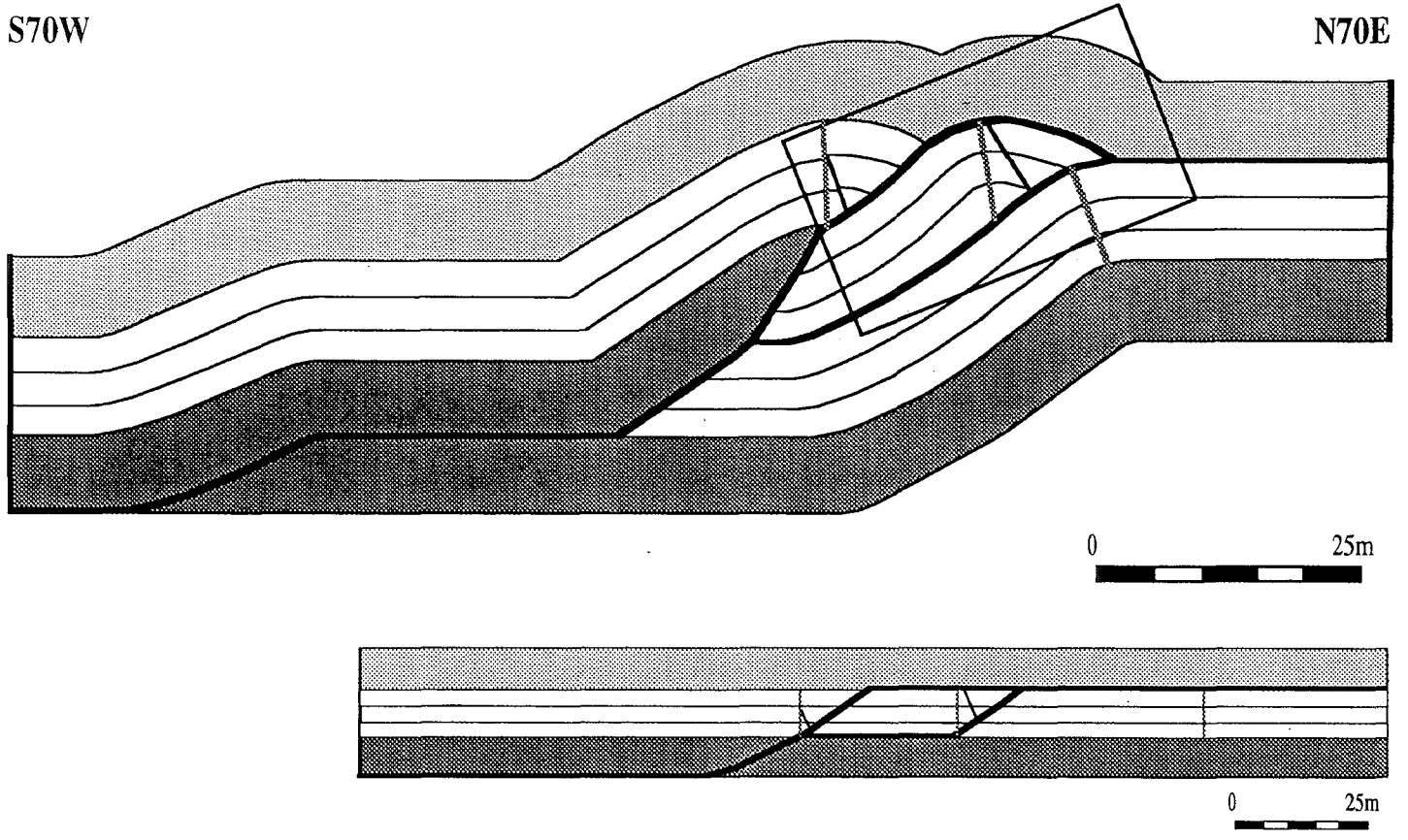

Figure 3. Bed-length and area balanced deformed- and restored-state cross sections of the Doublespring duplex. A regional dip of 25° to towards N70°E has been removed. Restored section is displayed at half-scale of the deformed section. Box indicates area shown in figure 8.

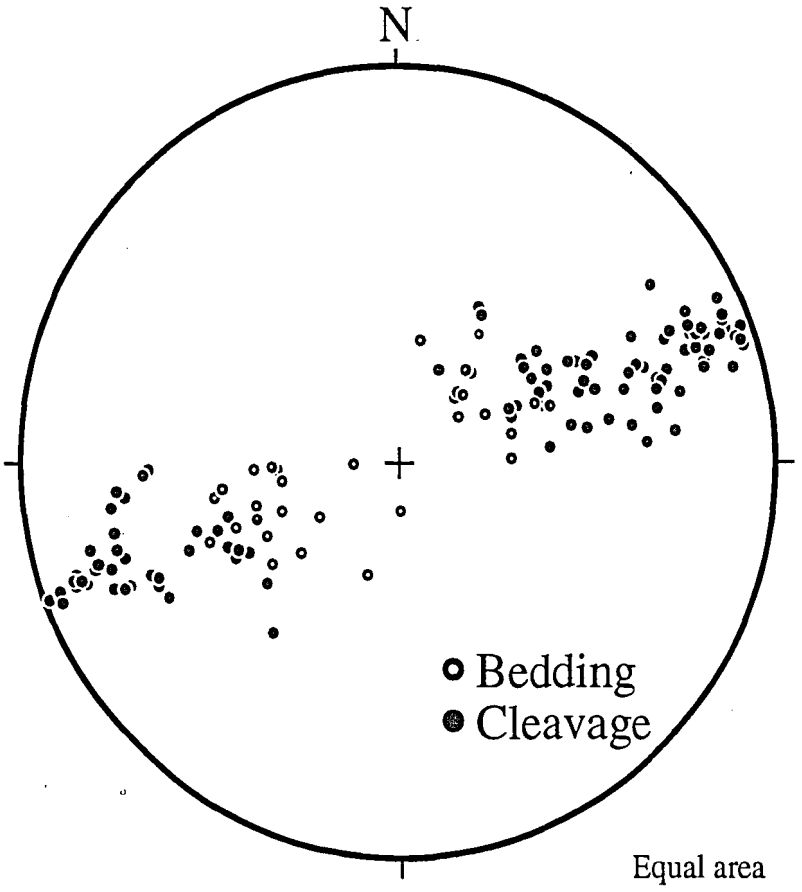

Figure 4. Equal area stereoplot of ploes to bedding (open circles) and cleavage (closed circles) in the Doublespring duplex. A narrow distribution of orientations shows that folds are approximately cylindrical in geometry.

lower hangingwall cutoffs have not been translated to the upper haningwall cutoffs, and is located at the top of the footwall ramp. The lower hangingwall cutoffs have been translated approximately 25 m beyond the upper footwall cutoffs in the middle fold such that the fold is located a relatively long distance away from it's footwall ramp. Antithetic reverse faults with minor displacement are formed at the leading edges of the upper and middle folds (Figs. 2 & 3). While the relationship of the lower fold to an underlying thrust is less constrained due to a lack of exposure, depth-to-detachment considerations, the axial surface orientation, and the continuation of the forelimb at regional orientation indicate that it is likely located at the top of an underlying footwall ramp. Alternatively, the lower fold may be a décollement fold. Thus each of the three folds have experienced a different structural evolution.

Bedding-parallel shear zones

A prominent feature in folds of the Doublespring duplex is the presence of relatively thin (5 cm to 1 m thick), widely spaced, recessive, bedding-parallel layers in the otherwise massive sequence of limestone. In contrast with the adjacent relatively undeformed layers, these layers are characterized by a penetrative pressure solution fabric spaced on the order of millimeters, refracted cleavage orientation, high finite strains, en-echelon extensional vein arrays, and layer-parallel shear surfaces (Fig. 5).

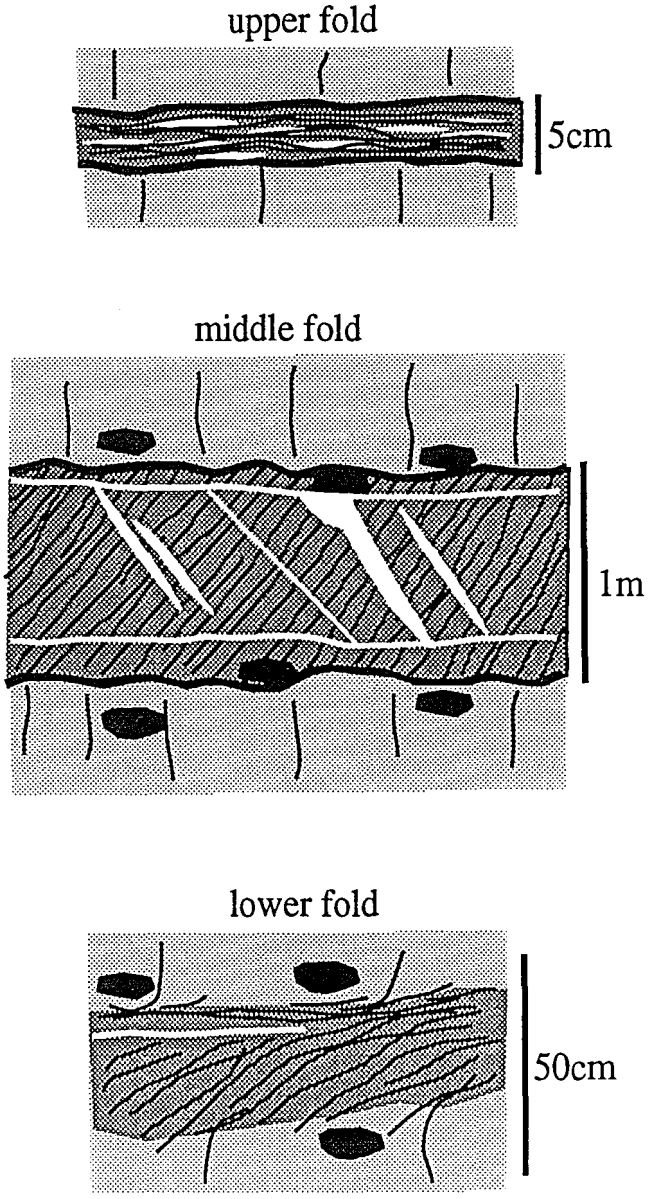

Figure 5. Sketches of representative shear zones from the upper, middle, and lower folds. Bedding is horizontal, protolith is shown in light gray, shear zones in dark gray, cleavage traces in black, chert nodules in black, and calcite veins in white in all cases. Note scales are not identical.

These features are interpreted to be bedding-parallel brittle-ductile shear zones (Ramsay and Graham, 1970). The shear zones are developed only on fold limbs, and grade laterally into massive layers where little fold-related strain has occurred (ie. above the décollement and at pinned fold hinges). Shear zones in the Doublespring structure may thus form from an initially massive protolith as a consequence of deformation associated with folding. The termination of shear zones near fold hinges generally occurs abruptly over less than 2-3 m, suggesting a steep strain gradient.

While shear zones in each of the folds share many common features, shear zones from each fold have characteristic features which are unique (Fig. 5). Shear zones in the upper fold have sharply defined bedding-parallel boundaries, range in thickness from 5 to 10 cm, and have an anastamosing bedding-parallel fabric consisting of a penetrative pressure solution cleavage with locally abundant cleavage-parallel extensional veins (Fig. 5a). Shear zones in the middle fold are characterized by sharply defined bedding-parallel boundaries, cleavage oriented approximately 45° from bedding and dipping away from the hinge, and locally well developed en-echelon vein arrays and bedding-parallel shear surfaces (Fig. 5b). The shear zone in the lower fold is characterized by diffuse boundaries, an anastamosing cleavage orientation ranging from approximately 45° steeper than bedding to bedding-parallel (Fig. 5c), and locally developed bedding-parallel shear surfaces and en-echelon extensional vein arrays. Where en-echelon vein arrays occur, they consistently indicate shear toward the fold

hinge. En-echelon veins and shear zone-bounding shear surfaces cross-cut cleavage and show no sign of internal pressure solution fabric development, suggesting a late-stage origin for these features.

The relatively thick layers between shear zones appear massive and undeformed in comparison. A weakly developed disjunctive cleavage (domains spaced on the order of tens of centimeters) is typically oriented at a steep angle to bedding in the massive layers forming a convergent fan, although isolated stylolites occur at almost any orientation. Extensional veins in massive layers are uncommon and show no systematic orientation.

The development of highly strained shear zones between relatively undeformed layers indicates inhomogeneous deformation where deformation is initially localized by heterogeneities in an otherwise isotropic material (Ramsay, 1982). Shear zones in all three folds form in a bed with relatively abundant black chert nodules measuring approximately 10 to 20 cm in diameter, which may have provided a mechanical discontinuity that could have initially localized deformation. The presence of relatively insoluble residue (ie. phylosilicates and Fe-oxides) in cleavage domains, fibrous overgrowths in pressure shadows, and both fibrous and sparry extensional veins indicate that pressure solution was a dominant deformation mechanism within the shear zones. Deformation may have also been localized in these layers because of a slightly higher detrital content or a finer matrix grain size, both of which would have increased

the pressure solution strain rate (Marshak and Engelder, 1985; Rutter, 1976). Once deformation commenced in the incipient shear zones, chemical and geometric strain softening by concentration and alignment of phyllosilicates allowed accumulation of large amounts of strain within the shear zones while adjacent rock experienced relatively little deformation.

INCREMENTAL STRAIN ANALYSIS

Displacement-controlled crystal fibers provide a continuous record of the incremental extension direction during mass transfer, and form the basis for a method to reconstruct incremental strain histories by measuring fiber trajectories (Elliott, 1972; Durney and Ramsay, 1973). Incremental strain histories recorded by displacement-controlled fibers have been instrumental in constraining the kinematics of deformation associated with cleavage development (Fisher, 1990), folding (Wickham and Anthony, 1977; Beutner and Diegel, 1985; Beutner *et al.,* 1988; Fisher and Anastasio, in press), and accretionary prism evolution (Sample and Fisher, 1986; Fisher and Byrne, 1992; Clark *et al.,* in press). Fibrous overgrowths in pressure shadows (Fig. 6a, b, & c) and fibrous extensional veins (Fig. 6d) are common in approximately 50% of the samples from shear zones in the Doublespring structure, and in less than 5% of the samples in

Figure 6a. Photomicrograph of calcite fibers on quartz-replaced crinoid ossicle. Curved fibers indicate a non-coaxial incremental strain history. Long axis of photo is parallel to cleavage. Field of view is approximately 1.0 millimeters.

Figure 6b. Photomicrograph of calcite fibers on quartz-replaced crinoid ossicle. Straight fibers indicate a coaxial incremental strain history. Long axis of photo is parallel to transport direction; view is cleavage-parallel (Z section). Field of view is approximately 1.0 millimeters.

Figure 6c. Photomicrograph of quartz fibers on framboidal pyrite. Curved fibers indicate a non-coaxial incremental strain history. Long axis of photo is parallel to cleavage. Field of view is approximately 0.5 millimeters.

Figure 6d. Photomicrograph antitaxial calcite veins. Curved fibers indicate a non-coaxial incremental strain history. Long axis of photo is parallel to cleavage. Field of view is approximately 1.0 millimeters.

the massive layers (two isolated samples adjacent to shear zones).

Fibers in pressure shadows are most commonly of calcite on host grains of quartz replaced bioclasts (Fig. 6a, b), although quartz fibers on framboidal pyrite also occur (Fig. 6c). Rf/ϕ analysis of crinoid ossicles in samples from shear zones indicates that bioclasts behaved as rigid porphyroclasts and have experienced little or no internal deformation. Sub-spherical quartz and pyrite host grains, fiber bundle shapes that approximate host grain boundary shapes, and curved fibers that are not always normal to growth interfaces indicate that fiber growth in pressure shadows was displacement-controlled (Ramsay and Huber, 1987).

Several observations indicate that fiber growth in pressure shadows was antitaxial (pyrite-type of Ramsay and Huber, 1987), occurring at the porphyroblast surface. Where the mineralogy of the fibers differs from that of the host grain, as in the Doublespring structure, fiber growth is generally antitaxial (Durney and Ramsay, 1973). Calcite fibers in optical continuity with matrix calcite, and fiber bundle shapes that generally parallel host grain boundaries are also indicative of antitaxial growth (Durney and Ramsay, 1973).

Straight displacement-controlled fiber trajectories indicate a coaxial incremental strain history, while curved fiber trajectories may result from a non-coaxial incremental strain history (ie. rotation of the incremental extension direction relative to the host grain), bending of initially straight fibers, or a combination of these factors. Optically

continuous and untwinned fibers, and fiber bundle shapes that parallel host grain boundaries indicate that curved fibers in samples from the duplex are largely undeformed (Durney and Ramsay, 1973; Ramsay and Huber, 1987; Fisher and Byrne, 1992), and thus represent a non-coaxial strain history.

Methods

Two types of methods exist for the reconstruction of incremental strain histories from syntectonic displacement-controlled fibers, those that apply an unstraining routine to correct for passive deformation of fibers (Ellis, 1987; Ramsay and Huber, 1987), and those that do not (Durney and Ramsay, 1973; Wickham, 1973). Durney and Ramsay's (1973) method was used in this study since fibers are interpreted to be largely undeformed, resulting in calculated incremental strain histories that are a direct representation of the fiber shape (Fisher and Byrne, 1992). To facilitate incremental strain history reconstruction, curved fiber trajectories can be approximated by a series of straight fiber segments representing coaxial increments separated by rigid rotations (Elliott, 1972). The orientation of each segment relative to a reference direction (ie. cleavage, bedding, or horizontal) records the orientation of the incremental extension direction, and the segment length normalized to the host grain radius represents the magnitude of incremental elongation. Incremental strain histories are measured from

fibrous veins in much the same way as from fibrous overgrowths, with the exception that elongation magnitudes are scaled to the width of wall rock domains between individual veins rather than to the host grain diameter. Incremental strain histories have been reconstructed for fibers viewed in both cleavage-parallel (Z), and fold axis-normal (Y) sections. Z sections are viewed looking down onto the cleavage plane, and Y sections are viewed towards N20°W (looking into the cross section).

The orientation and magnitudes of strain increments are conveniently displayed on cumulative incremental strain history (CISH) diagrams (Figs. 7 & 8) where the horizontal axis is orientation in degrees and the vertical axis represents the cumulative magnitude of incremental elongations. By convention (ie. Beutner and Diegel, 1985), clockwise is negative and counterclockwise is positive on CISH diagrams. The dip direction (also the projection of the inferred transport direction), N70°E, is used as a reference direction for analyses of cleavage-parallel Z sections (Fig. 7). Cleavage was used as a reference direction for all Y section analyses, and thus will always plot at 0° on CISH diagrams (Fig. 8). The orientations of bedding and horizontal are displayed on CISH diagrams for Y section analyses as dashed and dotted lines, respectively (Fig. 8). A vertical trajectory on a CISH diagram represents a coaxial strain history, a horizontal trajectory represents a rigid rotation of incremental extension direction relative to the host grain, and a sloping trajectory represents a non-coaxial strain history where the incremental extension direction is rotating relative to the host grain as strain

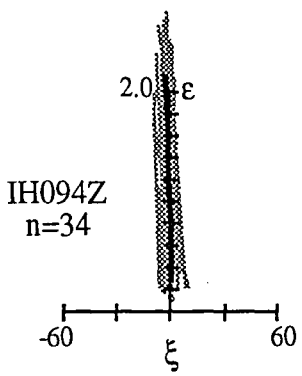

Figure 7. Cumulative incremental strain history (CISH) diagram for fibers in a cleavage-parallel (Z) section of sample IH094. The dip direction (also the inferred transport direction), N70°E, was used as a reference direction and plots at 0. A coaxial strain history in this orientation indicates coaxial downdip extension and plane-strain deformation in the direction of transport.

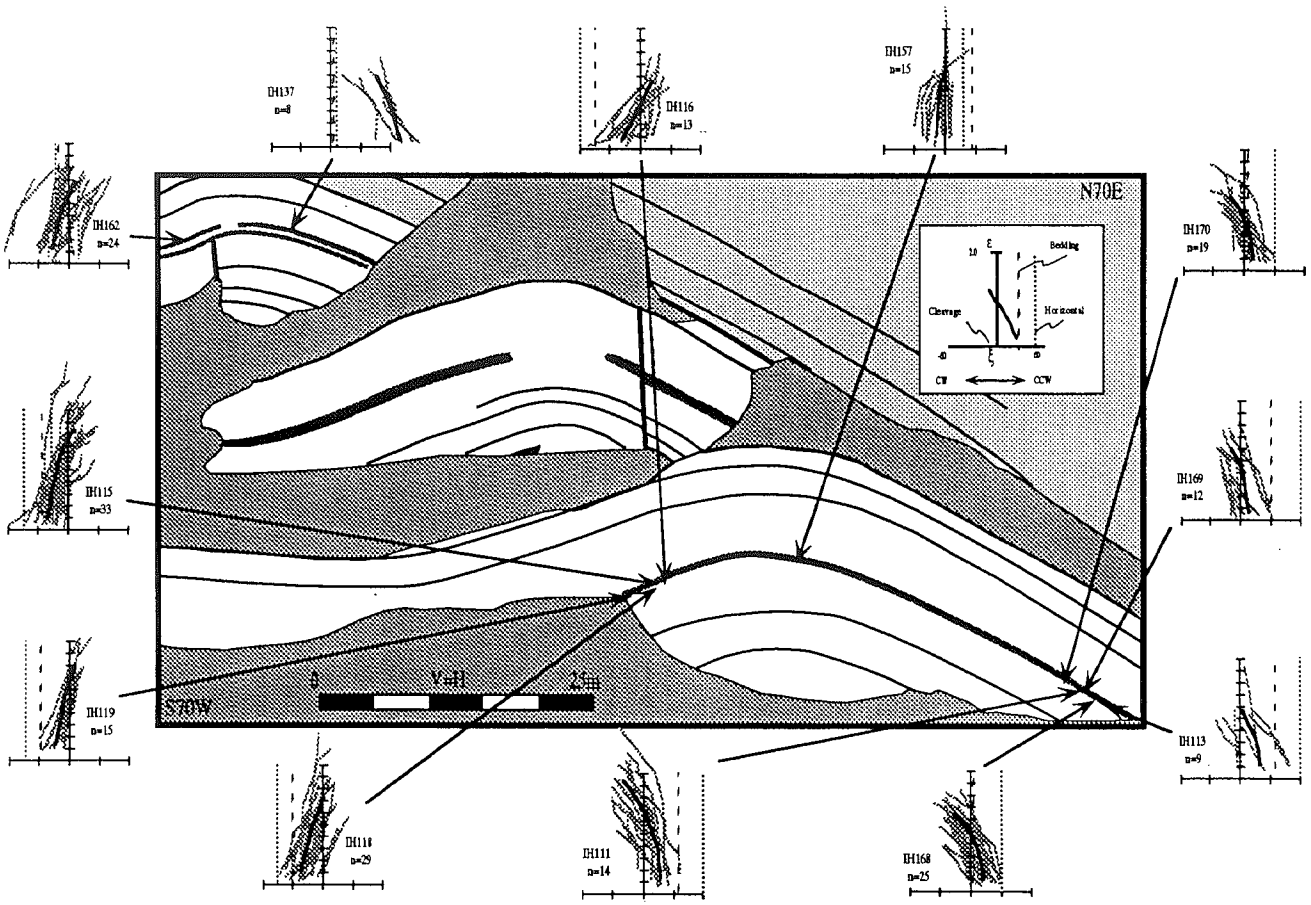

Figure 8a. Sketch of folds in the Doublespring duplex (see figures 2 & 3 for location). Shear zones are shown in dark grey, and massive layers in white. Cumulative incremental strain history (CISH) data is shown for samples from the upper and lower folds.

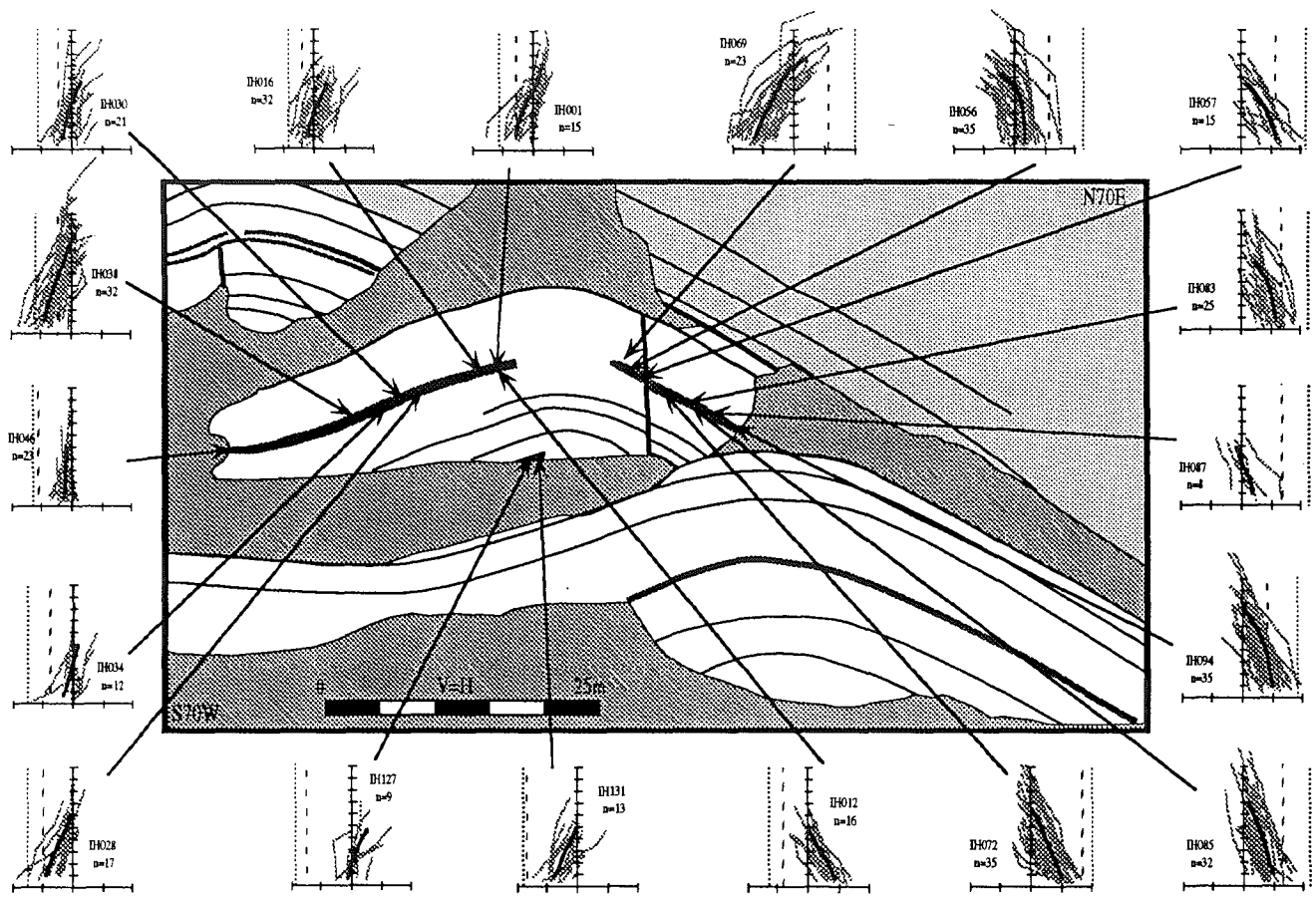

Figure 8b. Sketch of folds in the Doublespring duplex (see figures 2 & 3 for location). Shear zones are shown in dark grey, and massive layers in white. Cumulative incremental strain history (CISH) data is shown for samples from the middle fold.

accumulates. A clockwise rotation of the incremental extension direction relative to the host grain plots as a negative slope on a CIS diagram, while a counterclockwise rotation of the incremental extension direction relative to the host grain plots as a positive slope. Incremental strain histories for individual fibers are represented as thin grey lines on CISH diagrams. An 'average' incremental strain history for each sample is shown as a bold black line on CISH diagrams (Figs. 7 & 8), and is calculated through linear interpolation of points spaced along each individual curve normalized to the mean of the endpoint coordinates (Clark *et al.,* in press).

To minimize the effects of porphyroclast rotation, only fibers in pressure shadows adjacent to sub-spherical host grains were measured. Only the central fiber was measured from each pressure shadow, and recrystallized or otherwise deformed fibers were avoided.

Results

Incremental strain histories reconstructed from fibers in cleavage-parallel (Z) sections (Fig. 6b) are coaxial (Fig. 7), indicating that deformation was plane strain in the direction of transport. Fibers viewed in fold axis-normal Y sections are typically curved (Fig. 6a), yielding non-coaxial incremental strain histories. CISH diagrams for Y sections are shown in figures 8a & b.

Fibers in sample IH162 from the shear zone on the backlimb of the upper fold record a counterclockwise rotation of the incremental elongation direction as strain accumulates, where early increments are nearly bedding-parallel and the latest increments are oriented approximately 20° from bedding. The latest increments of fiber growth are nearly cleavage-parallel. Antitaxial fibrous extensional veins in a sample from the forelimb of the same shear zone (sample IH137) show the opposite sense of incremental extension direction rotation, with initial increments approximately 60° counterclockwise of bedding and later increments approximately 50° counterclockwise of bedding.

Samples from within shear zones on the backlimb of the middle fold (IH001, IH016, IH022, IH028, IH030, IH034, IH038, IH046, IH127, IH131, and IH150) show counterclockwise rotations of the incremental extension direction, with early fiber increments approaching bedding-parallel and the latest fiber increments at a steeper angle from bedding. The final increment of fiber growth for these samples is generally nearly parallel to cleavage. Sample IH012 is located below the upper shear zone and shows a clockwise rotation of the incremental extension direction, with early fiber increments approximately 60° from bedding and the latest increments approximately 25° from bedding. Samples from the shear zone on the forelimb of the middle fold (IH056, IH057, IH072, IH083, IH085, and IH087) show clockwise rotations of the incremental extension direction, with early fiber increments approximately bedding-

parallel, and the latest fiber increments at a steeper angle from bedding. Again, late fiber increments are close to cleavage-parallel. Sample IH069 is located immediately above the shear zone on the forelimb of the upper horse and shows a counterclockwise rotation of the incremental extension direction, with early fiber increments approximately 60° from bedding and the latest increments approximately 20° from bedding.

Shear zone samples from the backlimb of the lower fold (IH115, IH116, IH118, and IH119) show a counterclockwise rotation of the incremental extension direction relative to the host grain, with early fiber increments nearly bedding-parallel and the latest increments at 30° to 45° from bedding (Fig. 8a). Sample IH157, located near the axial surface of this fold, has fibers that record nearly coaxial elongation at an orientation 20° clockwise from bedding. Samples IH111, IH113, IH168, IH169, and IH170 from the forelimb of the lower horse contain fibers that record a clockwise rotation of the incremental extension direction relative to the host grain. Late fiber increments are nearly cleavage parallel for samples from the backlimb of the lower fold, and range from cleavage-parallel to clockwise of cleavage for forelimb samples.

Thus fibers in shear zone samples from all three folds record a reversal of fiber curvature near the fold hinge. Fibers in samples from outside of the shear zones curve the opposite sense from shear zone fibers on the same limb.

Interpretation

Non-coaxial strain histories recorded by crystal fibers are typically interpreted as resulting from either 1) rotation of the sample through an incremental extension direction fixed in space, or 2) progressive rotation of fiber increments during shear (Beutner and Diegel, 1985). In ideal bedding-parallel simple shear, the incremental extension direction is fixed at 45° from bedding such that fibers grow at 45° from bedding and are progressively swept towards parallelism with bedding. In samples from the bedding-parallel shear zones, late fiber increments are generally oriented at a moderate angle from bedding (25° to 55°), with earlier fiber increments progressively closer to parallel with bedding. This pattern of incremental strain histories is interpreted to be compatible with bedding-parallel shear. This interpretation is in agreement with textural evidence such as fabric orientation and en-echelon vein arrays which also suggest bedding-parallel shear. Fibers in sample IH137 record primarily bedding-normal extension with a small amount of rotation that is consistent with bedding-parallel shear. The shear sense recorded on each limb of all three folds is consistently toward the hinge, compatible with flexural flow towards a pin line located near the axial surface.

Pressure solution cleavage in limestones is generally defined by the concentration of relatively insoluble components in distinct domains or selveges, and is thus considered

to be dynamically unstable. Comparison of the relative orientations of cleavage and fibers allows determination of the timing of cleavage formation relative to the recorded strain history. A nearly cleavage-parallel orientation of the latest increments of fiber growth for samples from shear zones in the Doublespring duplex indicates that cleavage generally developed late in the strain history. This conclusion is different from other studies in similar rocks (Fisher and Anastasio, in press) where cleavage is found to track the long axis of the finite strain ellipsoid. This observation suggests that formation of a mesoscopic cleavage fabric may not occur until some finite amount of deformation has occurred.

The kinematics within massive layers between bedding-parallel shear zones is less well constrained, as only 5% of samples collected from these layers contain incremental strain indicators. Both of the samples from these layers containing incremental strain indicators (IH012 and IH069) are located adjacent to bedding parallel shear zones (within 5 cm), in narrow, local zones of intermediate fabric intensity. The early extension increments oriented at a high angle from bedding and later increments at a moderate to shallow angle from bedding recorded in these samples are not compatible with bedding parallel shear, and may instead be reflective of rotation through a fixed extension direction. The orientation of the extension direction, as indicated by the orientation of the final increments of fiber growth, is not the same for the two samples. Thus the kinematics of the massive layers can not be simply explained by rotation

through a common fixed extension direction, but may be a consequence of a more complex distribution of extension directions. More data is required to adequately constrain the kinematics of these layers.

DISCUSSION

Folding first versus faulting first

The relative timing of folding and faulting is of paramount importance in the evolution of fault-related folds, and is often ambiguous in natural structures (Dahlstrom, 1970). Several observations suggest that propagation of imbricate faults preceded folding in the Doublespring duplex. Because of the concentric nature of the folds in the Doublespring duplex, footwall synclines would be expected to exist if folding preceded faulting. The lack of a footwall syncline near the trailing edge of the horse (footwall for upper fold) suggests that faulting occurred before folding. Morphological differences between bedding-parallel shear zones in each of the folds suggest that they were likely structurally isolated by a fault when they developed. Since shear zone development is interpreted to be coincident with folding, this suggests that the thrust ramps formed prior to folding.

This conclusion is intuitively satisfying since failure criteria for fracturing and

buckling predict that massive layers are more likely to fail by faulting than buckling, other parameters equal. The faulting instability envelope (Drucker and Prager, 1952; Jamison, 1992) is independent of layer thickness, but the critical stress varies with the square of layer thickness for the buckling stability envelope (Tomishenko, 1936; Johnson and Page, 1976; Jamison, 1992) and thus would be high for a thick, massive unit such as the Scott Peak Formation. Thus folds in the Doublespring duplex are fundamentally different from folds that are interpreted to have formed by buckling before (Fischer *et al.,* 1992) or during faulting (Fisher and Anastasio, in press).

Kinematics of folding

The variation in spacing of and displacement on imbricates within the Doublespring duplex allow examination of folds related to different types of axial surfaces at various stages of development. When taken as an evolutionary sequence where the upper fold represents an early stage with little displacement and an axial surface fixed near the upper footwall cutoff and the middle fold represents a later stage with greater displacement and an axial surface fixed at the lower hangingwall cutoff, the fold geometries and axial surface relationships are suggestive of fault-bend folding with migrating axial surfaces (ie. Sanderson, 1982; Suppe, 1983). Shallow bed cutoff angles, open interlimb angles, and a fault-before-fold sequence of deformation are also

consistent with a fault-bend fold origin for folds in the Doublespring duplex. Kinematic models of parallel fault-bend folding (Sanderson, 1982; Suppe, 1983) predict specific senses and magnitudes of simple shear to occur at different times and locations through the evolution of the fold, including a shear reversal at the top of the footwall ramp (Fig. 9). While the observed incremental strain histories for folds in the Doublespring duplex are not incompatible with these predictions, many of the predicted shear events are not recorded. This suggests that either 1) not all of the shear events associated with fault-bend folding are recorded, or 2) the observed incremental strain histories and associated fabrics are not a consequence of passive fault-bend folding. Because folding at each of the axial surfaces occurred under similar physical conditions, it is unlikely that only selective events would be recorded. This suggests that the observed incremental strain histories are indeed reflective of folding about a fixed-hinge.

Recent studies have interpreted other asymmetric fault-related folds to have formed by folding about a fixed hinge based on the distribution of structural fabrics (Fischer *et al.*, 1992) and incremental strain histories (Fisher and Anastasio, in press). Incremental strain data from folds in the Doublespring duplex also suggest folding around a fixed hinge, but fixed-hinge folding on the ramp to the present amplitude is unlikely because of 1) the volume problem in the hinge area associated with fixed-hinge folding (Fig. 10a), and 2) the top-to-the hinterland shear in the thrust sheet required to preserve shallow hangingwall cutoffs and open interlimb angles (Fig. 10b). Fixed-

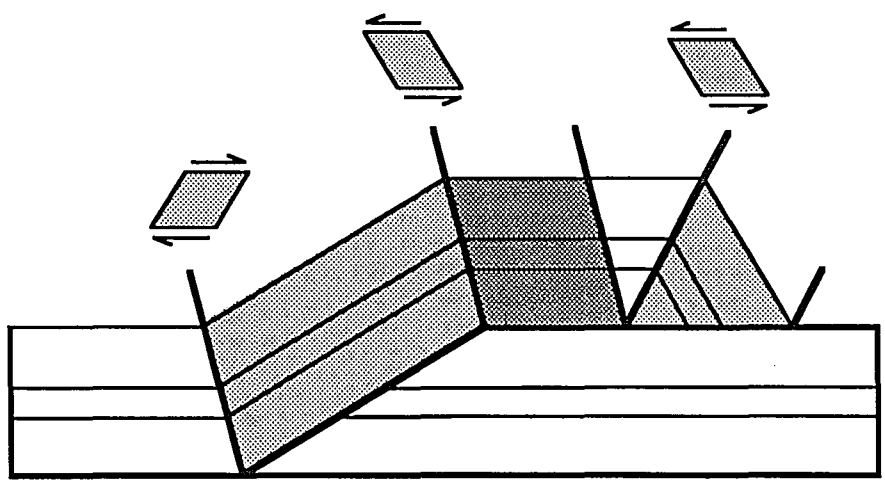

Figure 9. Distribution of bedding parallel simple shear predicted by Suppe's (1983) parallel model of fault-bend folding. Sense of shear at different axial surfaces is indicated by parallelograms and arrows. Unsheared domains are shown in white, once sheared domains in light grey, and twice sheared domains in dark grey. Note reversal of shear sense at top of footwall ramp.

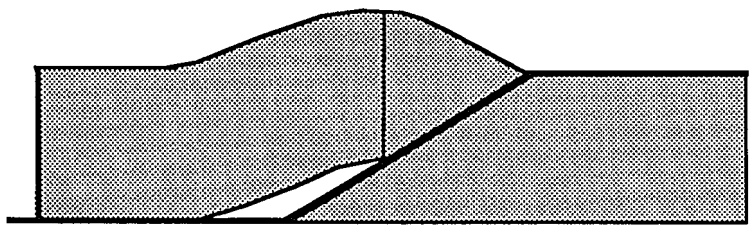

Figure 10a. Volume problem associated with fixed-hinge buckle folding. Excess cross sectional area must be accomodated by mass transfer or brecciation, or supported as an open void.

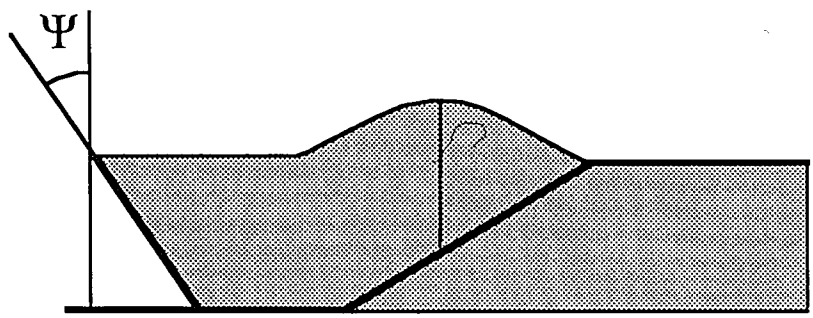

Figure 10b. Top-to-the-hinterland shear required to preserve shallow hangingwall cutoffs and open interlimb angle during fixed-hinge buckling. Amount of angular shear determined using bed-length balancing. Note that steeper hangingwall cutoffs and a tight interlimb angle are required to eliminate bulk shear of thrust sheet.

hinge folding creates a space problem in the core of the fold that must be accommodated by ductile flow or supported as an open volume. Although there is possible evidence for thickening in the unexposed core of the middle fold (Fig. 8), the magnitude is small and could simply be a consequence of the concentric fold geometry. Top-to-the hinterland shear accommodating folding is unlikely since shear zones are restricted to the limbs of anticlinal folds, suggesting a nearly vertical trailing edge loose line for the thrust sheet. A likely alternative is that the shear zones developed during a period of low-amplitude buckling about a fixed hinge such that the magnitudes of these problems would be minimized.

A fault-before-fold sequence suggests that the incremental strain history recorded by fibers occurred during low amplitude fixed-hinge buckle folding in response to resistance to initial translation of the thrust sheet up the ramp. Leading edge antithetic faulting in the upper folds also likely occured in response to resistance to translation up the ramps (ie. Serra, 1977).

Evolution of folds in the Doublespring duplex

Structural geometries, distributions of tectonic fabrics, and incremental strain histories suggest an evolutionary history for fault-related folds in the Doublespring duplex as follows. The structures originated when the imbricate thrust ramp formed in

response to a fracture instability (Fig. 11a). Increased stress caused by resistance to translation on the stepped fault surface caused low amplitude buckling of the thrust sheet and development of bedding-parallel shear zones (Fig. 11b). Fiber growth was contemporaneous with shear zone development, and it it this event that is recorded in the incremental strain histories. Because the pressure solution strain rate is known to be proportional to deviatoric stress (Rutter, 1976), the effectiveness of pressure solution as a deformation mechanism would have been enhanced during this period of elevated stress magnitudes. Low-amplitude buckling may have occurred at axial surfaces located on a ramp (upper fold), at the base of a ramp (middle fold), or away from a ramp (lower fold?). After the initial resistance to translation was overcome by buckling, thrust sheets were translated to form the present fold geometry by fault-bend folding (Fig. 11c). No textural record of translation or fault-bend folding exist, as indicated by the similarity in the kinematics of the folds despite their different translational histories and the fact that there is no textural record for folding at active or mobile axial surfaces. Strain is required to accommodate subsequent fault-bend folding, but is not recorded by any structural fabric. This indicates that strain accommodated by fault-bend folding occurred by a different mechanism, perhaps because these processes occurred under lower stress conditions.

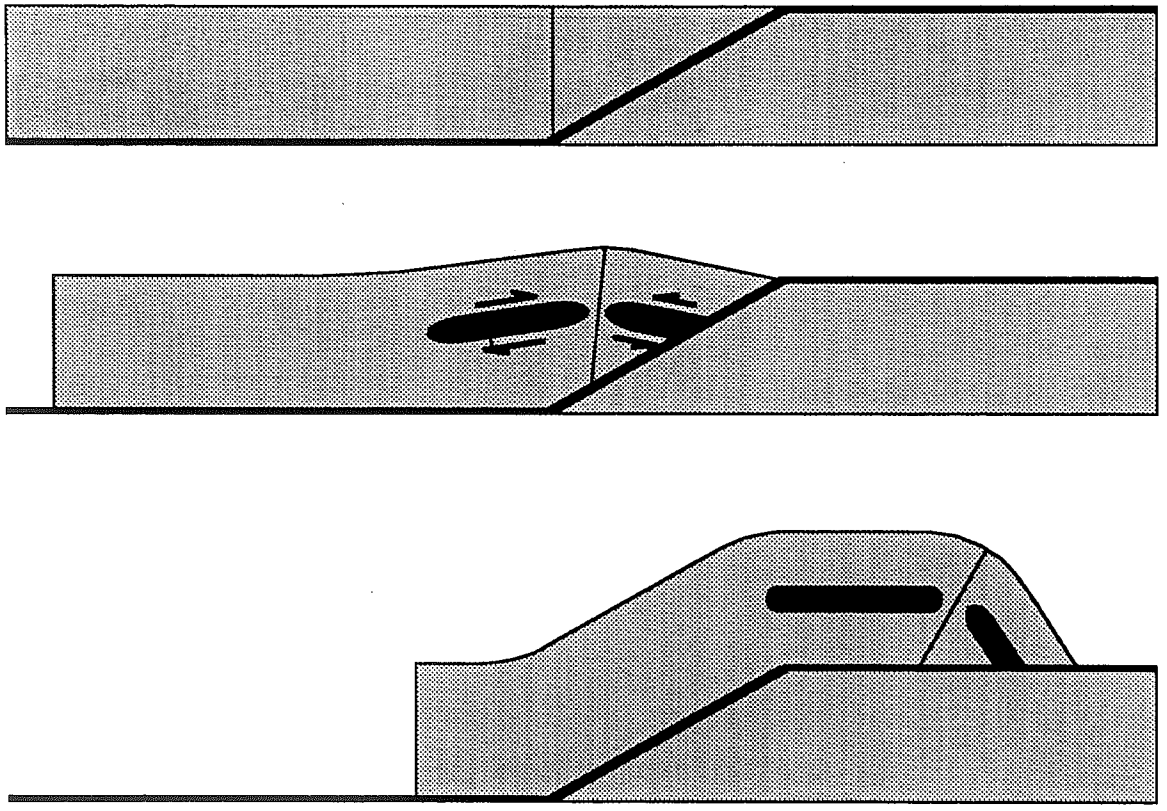

Figure 11. Kinematic evolution of fault related folds in the Doublespring duplex. Shear zones are highlighted in black, massive layers in grey. See text for description.

CONCLUSIONS

Analysis of the structural geometry, distribution of tectonic fabrics, and incremental strain data from the Doublespring duplex leads to several important conclusions about the structural evolution of fault-related folds.

1) No textural fabric is associated with propagation of faults, translation of the thrust sheet along a flat, or fault-bend folding, while shear zones and fibers in overgrowths and veins record a period of buckle folding. This suggests that the stress conditions may have been different during buckling and fault-bend folding.

2) Fibers record only the incremental strain history associated with buckle folding, and only in areas affected by mass transfer (ie. shear zones). Distributions of fabrics and incremental strain histories indicate that different layers experience different kinematic histories associated with folding. These data suggest flexural flow folding around a hinge near the axial surface of the fold occurred in bedding-parallel shear zones, and massive layers experienced rotation through a fixed, but not common, extension direction.

3) Cleavage in bedding-parallel shear zones forms late in the strain history, as indicated by late fiber increments that are nearly parallel to cleavage.

4) Fault-related folds may initiate in response to a fracture instability, like a fault-bend fold, and later experience fixed-hinge buckling in response to resistance to

translation.

REFERENCES

Baldwin, E. M. 1951. Faulting in the Lost River Range area of Idaho. *Am. J. Sci.* **249**, 884-902.

Beutner, E. C. & Diegel, F. 1985. Determination of fold kinematics from syntectonic fibers in pressure shadows, Martinsburg slate, New Jersey. *Am. J. Sci.* **285**, 16-50.

Beutner, E. C., Fisher, D. M. & Kirkpatrick, J. L. 1988. Kinematics of deformation as a thrust fault ramp (?) from syntectonic fibers in pressure shadows. In: *Geometries and mechanisms of thrusting, with special reference to the Appalachians* (edited by Mitra, G. & Wojtal, S.). *Spec. Pap. geol. Soc. Am.* **222**, 77-88.

Boyer, S. E. & Elliott, D. 1982. Thrust systems. *Bull. Am. Ass. Petrol. Geol.* **66**, 1196-1230.

Boyer, S. E. 1986. Styles of folding within thrust sheets: examples from the Appalachians and the Rocky Mountains of the USA and Canada. *J. Struct. Geol.* **8**, 325-339.

Clark, M. B., Fisher, D. M. &Chia-Yu, L. in press. Kinematic analysis of the Hshuehsan Range: A large-scale pop-up structure.*Tectonics.*

Crone, A. J. & Haller, K. M. 1991. Segmentation and the coseismic behavior of Basin and Range normal faults: examples from east-central Idaho and southwestern Montana, U.S.A. *J. Struct. Geol.* **13**, 151-164.

Dahlstrom, C. D. A. 1970. Structural geology in the eastern margin of the Canadian Rocky Mountains. *Bull. Can. Petrol. Geol.* **18**, 332-406.

Durney, D. W. & Ramsay, J. G. 1973. Incremental strains measured by syntectonic crystal growth. In: *Gravity and Tectonics* (edited by DeJong, K. A.). Wiley, 67-96.

Drucker, D. C. & Prager, W. 1952. Soil mechanics and plastic analysis for limited design. *Quart. of App. Math.* **10** 157-165.

Elliott, D. 1972. Deformation paths in structural geology. *Bull. geol. Soc. Am.* **83**, 2621-2638.

Ellis, M. A. 1987. The determination of progressive deformation histories from antitaxial syntectonic fibers. *J. Struct. Geol.* **8**, 701-709.

Fisher, D. M. 1990. Orientation history and rheology in slates, Kodiak and Afognak Islands, Alaska. *J. Struct. Geol.* **12**, 483-498.

Fisher, D. M. & Byrne, T. 1992. Strain variations in an ancient accretionary complex: Implication for forearc evolution. *Tectonics* **11**, 330-347.

Fisher, D. M. & Anastasio, D. J. in press, Kinematic analysis of a large-scale fault-propagation fold, Lost River Range, Idaho. *J. Struct. Geol.*

Fisher, M. P., Woodward, N. B. & Mitchell, M. M. 1992. The kinematics of break-thrust folds. *J. Struct. Geol.* **14**, 451-460.

Geiser, P. A. 1988. The role of kinematics in the construction and analysis of geological cross sections in deformed terranes. In: *Geometries and mechanisms of thrusting, with special reference to the Appalachians* (edited by Mitra, G. & Wojtal, S.). *Spec. Pap. geol. Soc. Am.* **222**, 47-76.

Jamison, W. R. 1987. Geometric Analysis of fold development in overthrust terranes. *J. Struct. Geol.* **9**, 207-219.

Jamison, W. R. 1992. Stress controls on fold thrust style. In: *Thrust Tectonics* (edited by McClay, K.R.), 155-164.

Johnson, A. M. & Page, B. M. 1976. A theory of concentric, kink, and sinusoidal folding and of monoclinal flexuring of compressible, elastic multilayers. VII. Development of folds within Huasna syncline, San Luis Obispo County, California. *Tectonophysics.* **37**, 97-143.

Knipe, R. J., 1985. Footwall geometry andthe rheology of thrust sheets. *J. Struct. Geol.* **7**, 1-10.

Mamet, B. L., Skipp, B., Sando, W. J. & Mapel, W. J. 1971. Biostratigraphy of Upper Mississippian ans associated Carboniferous rocks in south-central Idaho.

Bull. Am. Ass. Petrol. Geol. **55**, 20-33.

Mapel, W. J., Read, W. H. & Smith, R. K. 1965. Geologic map and sections of the Doublespring quadrangle, Custer and Lemhi Counties, Idaho. *U.S. Geol. Surv. Geol. Quad. Map.* **GQ-464.**

Marshak, S. and Engelder, T. 1985. Development of cleavage in limestones of a fold-thrust belt in eastern New York. *J. Struct. Geol.* **7**, 345-359.

Mitra, S. 1990. Fault-propagation folds: Geometry, kinematic evolution, and hydrocarbon traps. *Bull. Am. Ass. Petrol. Geol.* **74**, 921-945.

Ramsay, J. G. 1982. Rock ductility and its influence on the development of tectonic structures in mountain belts. In: *Mountain Building Processes* (edited by Hsü, K. J.). Academic Press,

Ramsay, J. G. & Graham, R. H. 1970. Strain variation in shear belts. *Can. J. Earth Sci.* **7**, 786-813.

Ramsay, J. G. & Huber, M. I. 1987. *The Techniques of Modern Structural Geology.* Vol. 1 & 2. Academic Press, New York.

Rich, R. L. 1934. Mechanics of low-angle overthrust faulting as illustrated by Cumberland thrust block, Virginia, Kentucky, and Tennessee. *Bull. Am. Ass. Petrol. Geol.* **18**, 1584-1596.

Rose, P. R. 1977. Mississippian carbonate shelf margins, western United States. *Wyoming Geological Association, 29th Annual Field Conference Guidebook* 155-

172.

Ross, C. P. 1947. Geology of the Borah Peak quadrangle, Idaho. *Bull. geol. Soc. Am.* **58**, 1085-1160.

Rutter, E. H. 1976. The kinetics of rock deformation by pressure solution. *Phil Trans. R. Soc. Lond.* **283**, 203-219.

Sample, J. C. & Fisher, D. M. 1986. Duplex accretion and underplating in an ancient accretionary complex, Kodiak Islands, Alaska. *Geology* **14**, 160-163.

Serra, S. 1977. Styles of deformation in the ramp regions of overthrusts faults. *Twenty-Ninth Annual Wyoming Geological Association Field Conference Guidebook.* 487-498.

Skipp, B., Sando, W. J. & Hall, W. E. 1979. The Mississippian and Pennsylvanian (Carboniferous) Systems in the United States-Idaho. *Prof. Pap. U.S. geol. Surv.* **1110-AA.**

Suppe, J. 1983. Geometry and kinematics of fault-bend folding. *Am. J. Sci.* **283**, 648-721.

Suppe, J. & Medwedeff, D. A. 1984. Fault-propagation folding. *Geol. Soc. Am. Abs. w. Progs.* **16.** 670.

Suppe, J. & Medwedeff, D. A. in press. Geometry and kinematics of fault-propagation folding. *Eclog. geol. Helv.* **83.**

Tomishenko, S.. 1936. *Theory of elastic stability.* McGraw Hill, New York.

Wickham, J. & Anthony, M. 1977. Strain paths and folding of carbonate rocks near Blue Ridge, central Appalachians. *Bull. geol. Soc. Am.* **88**, 920-924.

Wickham, J. S. 1973. An estimate of strain increments in a naturally deformed carbonate rock. *Am. J. Sci.* **273**, 23-47.

Willis, B. 1893, Mechanics of Appalachian structure. *U.S. Geological Survey Annual Report* 13 (1891-1892), part 2, 217-281.

VITA

Christopher Alan Hedlund was born in Chicago, Illinois on March 3rd, 1968 to Ronald P. and Cathy S. Hedlund. Chris grew up and was educated in Glenview, Illinois. He began stugying geology in an undergraduate program at the University of illinois at Urbana-Champaign. Chris graduated Magna Cum Laude from the University of Illinois with a B.S. degree in May, 1990. During the summer of 1990, he worked as a summer intern in an exploration group with Exxon, U.S.A. Chris entered the graduate program at Lehigh in September of 1990, where he was a Parkhurst Fellow for 2 semesters, a research assistant for 2 semesters, and a teaching assistant for one semester.

Publications:

Hedlund, C.A., Anastasio, D. J., and Fisher, D.M., *in prep.*, Kinematics of fault-related folding in a duplex, Lost River Range, Idaho, U.S.A., to be submitted to Journal of Structural Geology.

Hedlund, C.A. and Anastasio, D. J., 1992, Fold mechanism partitioning and kinematics of fault-bend folding in a duplex, Lost River Range, Idaho, Geological Society of America Abstracts with Programs, p. 246.

Hedlund, C.A., Anastasio, D. J., and Fisher, D.M., 1992, Folding and strain-induced layering in massive carbonates: Insights from the Lost River Range, Idaho, EOS, Trans. AGU, v.73, p. 280.

Krol, M., Gosse, J., Hedlund, C., *et al.*, 1992, 40Ar/39Ar constraints on the extent of both Paleozoic and Mesozoic thermal overprinting of Reading Prong basement adjascent to the Newark Basin, EOS, Trans. AGU, v.73, p. 279.

Hedlund, C.A., Gosse, J.C., Strasser, J.C., and Kodama, K.P., 1991, Mid-Jurassic synfolding magnetization of Newark Supergroup red sediments, Eastern PA, EOS, Trans. AGU, v.72, p. 128.

END

OF

TITLE